References

COX, J. M. (1967). *J. Mol. Biol.* **28**, 151–156.
DIAMOND, R. (1976). *Acta Cryst.* A**32**, 1–10.
DRESDEN, A. (1930). *Solid Analytical Geometry and Determinants*, p. 123. New York: John Wiley.
FERRO, D. R. & HERMANS, J. (1977). *Acta Cryst.* A**33**, 345–347.
FLIPPEN-ANDERSON, J. L. (1978). Private communication.
HENDRICKSON, W. A. & WARD, K. B. (1977). *J. Biol. Chem.* **252**, 3012–3018.
KABSCH, W. (1976). *Acta Cryst.* A**32**, 922–923.
MCLACHLAN, A. D. (1972). *Acta Cryst.* A**28**, 656–657.
NYBURG, S. C. (1974). *Acta Cryst.* B**30**, 251–253.
RAO, S. T. & ROSSMANN, M. G. (1973). *J. Mol. Biol.* **76**, 241–256.
ROSSMANN, M. G. & BLOW, D. M. (1962). *Acta Cryst.* **15**, 24–31.

Acta Cryst. (1979). A**35**, 163–170

X-ray Diffraction by Small Crystals

BY T. INO

Department of Physics, Osaka City University, Osaka, Japan

AND N. MINAMI

Department of Physics, Kinki University, Osaka, Japan

(*Received* 9 *April* 1976; *accepted* 1 *August* 1978)

Abstract

A general method of calculating the intensity of X-ray diffraction from small crystalline particles whose boundary is defined by a shape function is discussed. The intensity formula which is generally given by a double sum over the reciprocal-lattice points is simplified into the form of a single sum, using 'the random-shift treatment' which assumes that the position of the boundary relative to the crystal lattice varies at random from crystal to crystal. By the use of Fourier theorems, the intensity formulas are also converted into a single sum over the direct lattice. Although the electron distribution in the particle has been defined in various ways by the shape function, a more reasonable expression of the electron density appropriate to small crystals is introduced. The intensity formulas derived on the basis of the new form of the electron density are compared with other intensity formulas which have so far been proposed.

1. Introduction

The effect of the external shape and the size of a crystal on X-ray diffraction intensity was first dealt with by Laue (1936) for a parallelepiped crystal having N_i unit cells along the $\mathbf{a}_i$ axis ($i = 1, 2, 3$), for which the diffraction intensity is expressed as

$$I^L(\mathbf{b}) = |F(\mathbf{b})|^2 G(\mathbf{b}), \tag{1}$$

with

$$F(\mathbf{b}) = \sum_\alpha f_\alpha(\mathbf{b}) \exp(2\pi i \mathbf{b}\mathbf{r}_\alpha), \tag{2}$$

$$G(\mathbf{b}) = \frac{\sin^2 \pi N_1 \xi}{\sin^2 \pi\xi} \frac{\sin^2 \pi N_2 \eta}{\sin^2 \pi\eta} \frac{\sin^2 \pi N_3 \zeta}{\sin^2 \pi\zeta}, \tag{3}$$

where $F(\mathbf{b})$ is the structure factor, $G(\mathbf{b})$ the Laue function, $f_\alpha(\mathbf{b})$ the atomic scattering factor of the αth atom located at $\mathbf{r}_\alpha = x_\alpha \mathbf{a}_1 + y_\alpha \mathbf{a}_2 + z_\alpha \mathbf{a}_3$ and $\mathbf{b}$ the scattering vector expressed as $\mathbf{b} = \xi\mathbf{a}_1^* + \eta\mathbf{a}_2^* + \zeta\mathbf{a}_3^*$, $\mathbf{a}_i^*$ being the reciprocal vectors.

In order to treat small crystals of arbitrary shapes, Patterson (1939) and Ewald (1940) introduced the shape function $s(\mathbf{r})$ defined by

$$s(\mathbf{r}) = \begin{cases} 1 & \text{inside the crystal boundary} \\ 0 & \text{outside the crystal boundary} \end{cases} \tag{4}$$

and expressed the electron density in a small crystal as

$$\rho_e(\mathbf{r}) = \rho_\infty(\mathbf{r}) s(\mathbf{r}), \tag{5}$$

where $\rho_\infty(\mathbf{r})$ is the electron density of a perfectly periodic infinite crystal. As a Fourier transform of $\rho_e(\mathbf{r})$, the amplitude of X-rays diffracted by the crystal is given as

$$A_e(\mathbf{b}) = (1/v) \sum_{\mathbf{h}} F(\mathbf{h}) S(\mathbf{b} - \mathbf{h}) \tag{6}$$

0567-7394/79/010163-08$01.00

with

$$S(\mathbf{b}) = \int s(\mathbf{r}) \exp(2\pi i \mathbf{br}) d\mathbf{r}, \quad (7)$$

where $S(\mathbf{b})$ is the shape factor of the crystal, v the volume of the unit cell and $\mathbf{h} = h\mathbf{a}_1^* + k\mathbf{a}_2^* + l\mathbf{a}_3^*$ (h,k,l: integers).

Considering only one term in equation (6), James (1954) proposed, as an approximate intensity near point $\mathbf{h}$, the formula

$$I_e^J(\mathbf{b}) = (1/v)^2 |F(\mathbf{h})|^2 |S(\mathbf{b} - \mathbf{h})|^2. \quad (8)$$

Guinier (1963) expressed the electron density as

$$\rho_{eu}(\mathbf{r}) = \sum_{\mathbf{m}} \rho_e^{\text{cell}}(\mathbf{r} - \mathbf{m}) s(\mathbf{m}) \quad (9)$$

with

$$\rho_e^{\text{cell}}(\mathbf{r}) = \begin{cases} \rho_\infty(\mathbf{r}) & \text{inside the unit cell} \\ 0 & \text{outside the unit cell,} \end{cases} \quad (10)$$

where $\mathbf{m} = m_1\mathbf{a}_1 + m_2\mathbf{a}_2 + m_3\mathbf{a}_3$ (m_i: integer). Namely, $\rho_{eu}(\mathbf{r})$ is the electron density in all unit cells whose cell origins lie inside the boundary. He derived the amplitude of the form

$$A_{eu}(\mathbf{b}) = (1/v)\mathscr{F}_{eu}(b)\sum_{\mathbf{h}} S(\mathbf{b} - \mathbf{h}) \quad (11)$$

with

$$\mathscr{F}_{eu}(\mathbf{b}) = \int \rho_e^{\text{cell}}(\mathbf{r}) \exp(2\pi i \mathbf{br}) d\mathbf{r}, \quad (12)$$

and obtained the intensity formula

$$I_{eu}(\mathbf{b}) = (1/v)^2 |\mathscr{F}_{eu}(\mathbf{b})|^2 \sum_{\mathbf{h}} |S(\mathbf{b} - \mathbf{h})|^2, \quad (13)$$

by neglecting

$$\sum\sum_{h \neq h'} S(\mathbf{b} - \mathbf{h}) S^*(\mathbf{b} - \mathbf{h}').$$

Further, as an approximation for the region near point $\mathbf{h}$, he replaced $\mathscr{F}_{eu}(\mathbf{b})$ with $F(\mathbf{h})$ and proposed the intensity formula

$$I_{eu}^G(\mathbf{b}) = (1/v)^2 |F(\mathbf{h})|^2 \sum_{\mathbf{h}'} |S(\mathbf{b} - \mathbf{h}')|^2. \quad (14)$$

Hosemann & Bagchi (1962) expressed the electron density as

$$\rho_{au}(\mathbf{r}) = \sum_{\mathbf{m}} \rho_a^{\text{cell}}(\mathbf{r} - \mathbf{m}) s(\mathbf{m}), \quad (15)$$

with

$$\rho_a^{\text{cell}}(\mathbf{r}) = \sum_{\alpha}^{\text{cell}} U_\alpha(\mathbf{r} - \mathbf{r}_\alpha), \quad (16)$$

where $U_\alpha(\mathbf{r}')$ is the electron distribution function of the αth atom at $\mathbf{r}_\alpha$ in a unit cell, the origin of $\mathbf{r}'$ being taken at the center of the atom; the sum is taken over all the atoms in the unit cell. The function $\rho_{au}(\mathbf{r})$ represents all electron distribution belonging to all the atoms in those unit cells whose cell origins are contained within the boundary. They derived the amplitude of the form

$$A_{au}(\mathbf{b}) = (1/v)F(\mathbf{b}) \sum_{\mathbf{h}} S(\mathbf{b} - \mathbf{h}), \quad (17)$$

from which, by the method of the ξ average (as so-called by them), they obtained the intensity formula

$$I_{au}(\mathbf{b}) = (1/v)^2 |F(\mathbf{b})|^2 \sum_{\mathbf{h}} |S(\mathbf{b} - \mathbf{h})|^2. \quad (18)$$

In their final intensity formula, they replaced $F(\mathbf{b})$ by $F(\mathbf{h})$ and put it inside the summation as

$$I_{au}^{HB}(\mathbf{b}) = (1/v)^2 \sum_{\mathbf{h}} |F(\mathbf{h}) S(\mathbf{b} - \mathbf{h})|^2. \quad (19)$$

For an extremely large crystal, since $S(\mathbf{b})$ approaches the δ function $\delta(\mathbf{b})$, I_e^J, I_{eu}^G and I_{au}^{HB} give the same result. For a very small crystal, however, they show intensity distributions substantially different from one another because $S(\mathbf{b})$ has a relatively broad distribution near $\mathbf{b} = 0$. Further, as will be pointed out in the next section, the electron distributions represented by the functions ρ_e, ρ_{eu} and ρ_{au} are too artificial to be appropriate to very small crystals. In this respect, therefore, a new function ρ_a is introduced in the present study. It is shown that ρ_a may be a more realistic model of electron distributions for very small crystals. Intensity formulas corresponding to ρ_e, ρ_{eu}, ρ_{au} and ρ_a are derived by the use of 'the random-shift treatment'. Calculations are performed either by the reciprocal-lattice sum or by the direct-lattice sum. The results obtained are compared and critically discussed.

2. Four kinds of electron density expression for a bounded crystal

The electron density for a bounded crystal is characterized by the shape function $s(\mathbf{r})$. The $s(\mathbf{r})$ in equation (5) cut the finite part defined by the boundary from the infinite distribution of the electron density $\rho_\infty(\mathbf{r})$, while $s(\mathbf{m})$ in equations (9) and (15) bounds the summation range of $\mathbf{m}$. On the other hand, the new density distribution $\rho_a(\mathbf{r})$ which is now introduced can be characterized by saying that it is concerned not with lattice points but with atoms which lie inside the boundary. Namely, $\rho_a(\mathbf{r})$ can be expressed as

$$\rho_a(\mathbf{r}) = \sum\sum_{\mathbf{m}\,\alpha} U_\alpha(\mathbf{r} - \mathbf{m} - \mathbf{r}_\alpha) s(\mathbf{m} + \mathbf{r}_\alpha). \quad (20)$$

The characteristic features of the four density functions, ρ_e, ρ_{eu}, ρ_{au} and ρ_a, are shown schematically in Fig. 1 for a two-dimensional hexagonal crystal having a circular boundary, assuming that each unit cell con-

tains two different atoms. These electron distributions differ from one another only near the boundary. However, since as seen in Fig. 1(*a*) the distribution represented by ρ_e does not keep the integrity of the electron cloud belonging to each atom, it is clear that $\rho_e(\mathbf{r})$ can hardly be a realistic electron distribution. The same also holds for ρ_{eu} (Fig. 1*b*). In addition, ρ_{eu} for a given shape function is accompanied by arbitrariness because ρ_{eu} depends on the choice of the unit cell in the crystal concerned. As for ρ_{au}, although the integrity of the electron cloud about each atom is not destroyed, it is also accompanied by the arbitrariness due to the choice of the unit cell. On the other hand, the density function ρ_a represents an electron distribution consisting of whole atoms, and is independent of the choice of the unit cell. Compared with the other density functions, therefore, ρ_a may reproduce most reasonably and realistically the electron distribution in a very small crystal corresponding to a given shape function.

It can be easily understood that there are the following relations between $\rho_\infty(\mathbf{r})$, $\rho_e^{\text{cell}}(\mathbf{r})$, $\rho_a^{\text{cell}}(\mathbf{r})$ and $U_\alpha(\mathbf{r}')$:

$$\rho_\infty(\mathbf{r}) = \sum_{\mathbf{m}} \rho_e^{\text{cell}}(\mathbf{r}-\mathbf{m}) = \sum_{\mathbf{m}} \rho_a^{\text{cell}}(\mathbf{r}-\mathbf{m}) = \sum_{\mathbf{m}}\sum_{\alpha} U_\alpha(\mathbf{r}-\mathbf{m}-\mathbf{r}_\alpha). \tag{21}$$

Using the crystal lattice function as

$$z(\mathbf{r}) = \sum_{\mathbf{m}} \delta(\mathbf{r}-\mathbf{m}), \tag{22}$$

and the relation $s(\mathbf{m}) = \int s(\mathbf{r})\delta(\mathbf{r}-\mathbf{m})\mathrm{d}\mathbf{r}$, one can transform $\rho_{eu}(\mathbf{r})$ into a convolution form as follows:

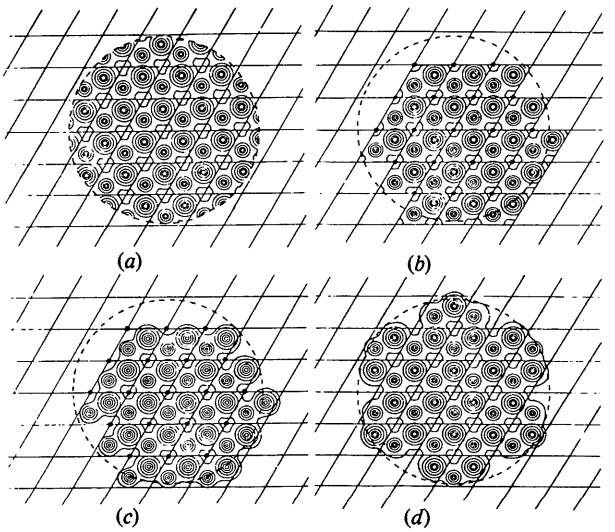

Fig. 1. Electron density maps of (*a*) ρ_e, (*b*) ρ_{eu}, (*c*) ρ_{au} and (*d*) ρ_a for a disk-shaped crystal. Broken lines show the boundaries specified by the shape function.

$$\rho_{eu}(\mathbf{r}) = \sum_{\mathbf{m}} \rho_e^{\text{cell}}(\mathbf{r}-\mathbf{m})s(\mathbf{m}) = \sum_{\mathbf{m}} \int \rho_e^{\text{cell}}(\mathbf{r}-\mathbf{r}')\delta(\mathbf{r}'-\mathbf{m})s(\mathbf{r}')\mathrm{d}\mathbf{r}' = \int \rho_e^{\text{cell}}(\mathbf{r}-\mathbf{r}')z(\mathbf{r}')s(\mathbf{r}')\mathrm{d}\mathbf{r}' = \rho_e^{\text{cell}}(\mathbf{r}) * [z(\mathbf{r})s(\mathbf{r})],$$

where $g_1(\mathbf{r}) * g_2(\mathbf{r})$, a convolution of $g_1(\mathbf{r})$ and $g_2(\mathbf{r})$, is defined as

$$g_1(\mathbf{r}) * g_2(\mathbf{r}) = \int g_1(\mathbf{r}-\mathbf{r}')g_2(\mathbf{r}')\mathrm{d}\mathbf{r}'. \tag{23}$$

Similarly, $\rho_e(\mathbf{r})$, $\rho_{au}(\mathbf{r})$ and $\rho_a(\mathbf{r})$ can be transformed into their convolution forms as follows:

$$\rho_e(\mathbf{r}) = \sum_{\alpha} [U_\alpha(\mathbf{r}) * z(\mathbf{r}-\mathbf{r}_\alpha)]s(\mathbf{r}) \text{ (PEJ)} \tag{24}$$

(Patterson, 1939; Ewald, 1940; James, 1954),

$$\rho_{eu}(\mathbf{r}) = \rho_e^{\text{cell}}(\mathbf{r}) * [z(\mathbf{r})s(\mathbf{r})] \text{ (G) (Guinier, 1963)} \tag{25}$$

$$\rho_{au}(\mathbf{r}) = \rho_a^{\text{cell}}(\mathbf{r}) * [z(\mathbf{r})s(\mathbf{r})] \text{ (HB) (Hosemann \& Bagchi, 1962)} \tag{26}$$

$$\rho_a(\mathbf{r}) = \sum_{\alpha} U_\alpha(\mathbf{r}) * [z(\mathbf{r}-\mathbf{r}_\alpha)s(\mathbf{r})] \text{ (IM) (this work).} \tag{27}$$

3. X-ray diffraction amplitude for a bounded crystal

The amplitude, $A(\mathbf{b})$, of diffracted X-rays is given by the Fourier transform of the electron density function $\rho(\mathbf{r})$, *i.e.*

$$A(\mathbf{b}) = \mathbf{F}\rho(\mathbf{r}) = \int \rho(\mathbf{r}) \exp(2\pi i \mathbf{br})\mathrm{d}\mathbf{r}. \tag{28}$$

By use of the convolution theory,

$$\mathbf{F}[g_1(\mathbf{r}) * g_2(\mathbf{r})] = \mathbf{F}g_1(\mathbf{r}) . \mathbf{F}g_2(\mathbf{r}), \tag{29}$$

$$\mathbf{F}[g_1(\mathbf{r}) . g_2(\mathbf{r})] = \mathbf{F}g_1(\mathbf{r}) * \mathbf{F}g_2(\mathbf{r}), \tag{30}$$

four $A(\mathbf{b})$'s corresponding to ρ_e, ρ_{eu}, ρ_{au} and ρ_a can be derived:

$$A_e(\mathbf{b}) = \sum_{\alpha} [\mathbf{F}U_\alpha(\mathbf{r}) . \mathbf{F}z(\mathbf{r}-\mathbf{r}_\alpha)] * \mathbf{F}s(\mathbf{r}) \text{ (PEJ),} \tag{31}$$

$$A_{eu}(\mathbf{b}) = \mathbf{F}\rho_e^{\text{cell}}(\mathbf{r}) . [\mathbf{F}z(\mathbf{r}) * \mathbf{F}s(\mathbf{r})] \text{ (G),} \tag{32}$$

$$A_{au}(\mathbf{b}) = \mathbf{F}\rho_a^{\text{cell}}(\mathbf{r}) . [\mathbf{F}z(\mathbf{r}) * \mathbf{F}s(\mathbf{r})] \text{ (HB),} \tag{33}$$

$$A_a(\mathbf{b}) = \sum_{\alpha} \mathbf{F}U_\alpha(\mathbf{r}) . [\mathbf{F}z(\mathbf{r}-\mathbf{r}_\alpha) * \mathbf{F}s(\mathbf{r})] \text{ (IM).} \tag{34}$$

Fourier transforms and convolutions of the functions concerned are

$$\mathbf{F}U_\alpha(\mathbf{r}) = f_\alpha(\mathbf{b}), \quad \mathbf{F}s(\mathbf{r}) = S(\mathbf{b}), \tag{35}$$

$$\mathbf{F}z(\mathbf{r}-\mathbf{d}) = (1/v)\exp(2\pi i \mathbf{bd}) \sum_{\mathbf{h}} \delta(\mathbf{b}-\mathbf{h}), \tag{36}$$

and then

$$\mathbf{F}z(\mathbf{r}-\mathbf{d}) * \mathbf{F}s(\mathbf{r}) = (1/v) \sum_{\mathbf{h}} \exp(2\pi i \mathbf{hd})S(\mathbf{b}-\mathbf{h}). \tag{37}$$

Thus, four $A(\mathbf{b})$'s can be rewritten as a reciprocal-lattice sum:

$$A(\mathbf{b}) = \sum_{\mathbf{h}} \Phi(\mathbf{b},\mathbf{h}) = (1/v) \sum_{\mathbf{h}} S(\mathbf{b}-\mathbf{h})\mathscr{F} \tag{38}$$

with

$$\mathscr{F}_e(\mathbf{h}) = \sum_{\alpha} f_\alpha(\mathbf{h}) \exp(2\pi i \mathbf{h}\mathbf{r}_\alpha) = F(\mathbf{h}) \text{ (PEJ)}, \tag{39}$$

$$\mathscr{F}_{eu}(\mathbf{b}) = \int \rho_e^{\text{cell}}(\mathbf{r}) \exp(2\pi i \mathbf{b}\mathbf{r}) d\mathbf{r} = \sum_{\mathbf{h}} F(\mathbf{h}) H(\mathbf{b}-\mathbf{h}) \text{ (G)}, \tag{40}$$

$$\mathscr{F}_{au}(\mathbf{b}) = \int \rho_a^{\text{cell}}(\mathbf{r}) \exp(2\pi i \mathbf{b}\mathbf{r}) d\mathbf{r} = \sum_{\alpha} f_\alpha(\mathbf{b}) \exp(2\pi i \mathbf{b}\mathbf{r}_\alpha) = F(\mathbf{b}) \text{ (HB)}, \tag{41}$$

$$\mathscr{F}_a(\mathbf{b},\mathbf{h}) = \sum_{\alpha} f_\alpha(\mathbf{b}) \exp(2\pi i \mathbf{h}\mathbf{r}_\alpha) = F(\mathbf{b},\mathbf{h}) \text{ (IM)}, \tag{42}$$

where

$$H(\mathbf{b}-\mathbf{h}) = e^{\pi i(\xi+\eta+\zeta)} \frac{\sin(\pi\xi)}{\pi(\xi-h)} \frac{\sin(\pi\eta)}{\pi(\eta-k)} \frac{\sin(\pi\zeta)}{\pi(\zeta-l)}. \tag{43}$$

Equations (39), (40) and (41) are identical with (6), (11) and (17) respectively. For $\mathbf{b} = \mathbf{h}$, these four $\mathscr{F}$'s are all equal to $F(\mathbf{h})$ but they generally differ from one another. $\mathscr{F}_e$, $\mathscr{F}_{au}$ and $\mathscr{F}_a$ can easily be calculated from atomic scattering factors, while $\mathscr{F}_{eu}$ needs complicated calculations including integrals or series.

For comparison, $\mathscr{F}(\xi 00)/(nZ)$, where Z is the atomic number and n the number of atoms in a unit cell, is calculated in the cases of monatomic s.c. (simple cube), b.c.c. and f.c.c. with $a = 4$ Å, by the use of an approximate expression, $f(\xi 00)$, given by

$$f(\xi 00) = \frac{Z}{1+\gamma(\xi/a)^2} = Z\varphi(\xi), \tag{44}$$

where

$$\varphi(\xi) = \alpha^2/(\alpha^2+\xi^2), \tag{45}$$

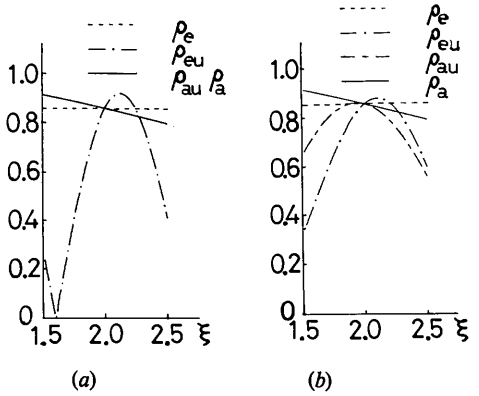

Fig. 2. Comparison among $\mathscr{F}$'s of four types. (*a*) $|\mathscr{F}|/Z$ for s.c. and (*b*) $|\mathscr{F}|/(nZ)$ for b.c.c. and f.c.c.

with $\alpha^2 = a^2/\gamma$. We obtain:

for s.c.

$$\left.\begin{aligned} &\mathscr{F}_e(h00)/Z = \varphi(h) \text{ (PEJ)},\\ &\mathscr{F}_{eu}(\xi 00)/Z = \varphi(\xi)[\cos(\pi\xi) + (\xi/\alpha)\sin(\pi\xi)]e^{\pi i\xi} \text{ (G)},\\ &\mathscr{F}_{au}(\xi 00)/Z = \mathscr{F}_a(\xi 00,h00) = \varphi(\xi) \text{ (HB and IM)}; \end{aligned}\right\} \tag{46}$$

for b.c.c. and f.c.c. (the same for both)

$$\left.\begin{aligned} &\mathscr{F}_e(h00)/(nZ) = \varphi(h) \text{ for } h \text{ even } (=0 \text{ for } h \text{ odd}) \text{ (PEJ)},\\ &\mathscr{F}_{eu}(\xi 00)/(nZ) = \varphi(\xi)\cos\left(\frac{\pi\xi}{2}\right)\left[\cos\left(\frac{\pi\xi}{2}\right) + \frac{\xi}{\alpha}\sin\left(\frac{\pi\xi}{2}\right)\right]e^{\pi i\xi} \text{ (G)},\\ &\mathscr{F}_{au}(\xi 00)/(nZ) = \varphi(\xi)\cos\left(\frac{\pi\xi}{2}\right)e^{(\pi i\xi/2)} \text{ (HB)},\\ &\mathscr{F}_a(\xi 00,h00)/(nZ) = \varphi(\xi) \text{ for } h \text{ even } (=0 \text{ for } h \text{ odd}) \text{ (IM)}; \end{aligned}\right\} \tag{47}$$

where the formulas (*B*1), (*B*2) in Appendix *B* are used for calculating $\mathscr{F}_{eu}(\xi 00)$. Curves for these $|\mathscr{F}|/(nZ)$ are shown in Fig. 2(*a*) for s.c. and in Fig. 2(*b*) for b.c.c. and f.c.c. where $\gamma = 2/3$ Å^2 and hence $\alpha^2 = 24$ are used.

4. Four types of intensity formulas and approximate forms

The intensity of X-rays diffracted by a bounded crystal is derived from equation (38) as

$$I(\mathbf{b}) = A(\mathbf{b})A^*(\mathbf{b}) = \sum_{\mathbf{h}} |\Phi(\mathbf{b},\mathbf{h})|^2 + \sum_{\mathbf{h}} \sum_{\mathbf{h}\neq\mathbf{h}'} \Phi(\mathbf{b},\mathbf{h})\Phi^*(\mathbf{b},\mathbf{h}'). \tag{48}$$

On deriving $I_e^J(\mathbf{b})$ in equation (8) and $I_{eu}(\mathbf{b})$ in equation (13), James and Guinier neglected the contribution from the last term in equation (48), considering that the overlap of two Φ's with different $\mathbf{h}'$ is small so that the last term may be negligible. Such a consideration, however, turns out to be invalid for very small crystals. Hosemann & Bagchi eliminated this term by using the method of 'ξ-average'. On the other hand, this term can also be eliminated by the use of 'the random-shift treatment' method. This method is adopted throughout the present paper. As described in Appendix *A*, it is assumed in this treatment that the position of the crystal boundary relative to the crystal lattice varies at random and the intensity average over such random shifts gives the intensity observed from the crystal powder sample.

From $A(\mathbf{b})$ in equation (38) and the $\mathscr{F}$'s in equations (39)–(42), therefore, the following four types of intensity formula can be derived:

$$I_e(\mathbf{b}) = (1/v)^2 \sum_{\mathbf{h}} |F(\mathbf{h})S(\mathbf{b}-\mathbf{h})|^2 \,[= I_{au}^{HB}(\mathbf{b})] \text{ (PEJ)}, \quad (49)$$

$$I_{eu}(\mathbf{b}) = (1/v)^2 |\mathscr{F}_{eu}(\mathbf{b})|^2 \sum_{\mathbf{h}} |S(\mathbf{b}-\mathbf{h})|^2 \text{ (G)}, \quad (50)$$

$$I_{au}(\mathbf{b}) = (1/v)^2 |F(\mathbf{b})|^2 \sum_{\mathbf{h}} |S(\mathbf{b}-\mathbf{h})|^2 \text{ (HB)}, \quad (51)$$

$$I_a(\mathbf{b}) = (1/v)^2 \sum_{\mathbf{h}} |F(\mathbf{b},\mathbf{h})S(\mathbf{b}-\mathbf{h})|^2 = I_a^{IM}(\mathbf{b}) \text{ (IM)}, \quad (52)$$

where equations (50) and (51) are identical to (13) and (18) respectively.

Hosemann & Bagchi replaced $F(\mathbf{b})$ by $F(\mathbf{h})$ in their equation (51) and put it inside the summation over $\mathbf{h}$ as in their final form $I_{au}^{HB}(\mathbf{b})$ in equation (19) which is identical to equation (49). In other words, they at first adopted $\rho_{au}(\mathbf{r})$ as the electron density function but finally replaced $\rho_{au}(\mathbf{r})$ by $\rho_e(\mathbf{r})$. As will be seen later, $I^{\mathrm{L}}(\mathbf{b})$ in equation (1) derived by Laue is found to be a special case of $I_{au}(\mathbf{b})$ for a parallelepiped crystal [see equation (55)].

An approximate form near point $\mathbf{h}$ in equation (8) derived by James is identical with a single term $\mathbf{h}$ in the summation of equation (49). Another approximate form of equation (14) derived by Guinier is obtained from $I_{eu}(\mathbf{b})$ in equation (50) by replacing $\mathscr{F}_{eu}(\mathbf{b})$ with $F(\mathbf{h})$. This replacement means, as seen in Fig. 2(*a*), (*b*), that the hill-shape curve with a peak shift from $\xi = 2$ is replaced by a straight line. Such a replacement may not be allowed for a very small crystal.

Since $S(\mathbf{b})$ is a maximum at $\mathbf{b} = 0$ and appreciable in the volume of the order of $1/V$ (V is the volume of the crystal) around $\mathbf{b} = 0$ and $\mathscr{F}$'s are generally different from one another except for $\mathbf{b} = \mathbf{h}$, the differences between I_e $(= I_{au}^{HB})$, I_{eu}, I_{au}, I_a^{IM}, I_e^J and I_{eu}^G become more appreciable as the crystal size becomes smaller, though they are all equal to $(V/v)^2 |F(\mathbf{h})|^2$ at $\mathbf{b} = \mathbf{h}$.

5. Four types of intensity formulas and two approximate forms

In order to compare four types of intensity formulas, I_e $(= I_{au}^{HB})$, I_{eu}, I_{au}, and I_a^{IM}, and also two approximate forms, I_e^J and I_{eu}^G, they are calculated for a parallelepiped crystal having N_i unit cells along the $\mathbf{a}_i$ axis. In this case, the shape factor $S(\mathbf{b}-\mathbf{h})$ in equation (7) can easily be calculated as

$$(1/v)^2 |S(\mathbf{b}-\mathbf{h})|^2 = G(\mathbf{b})|H(\mathbf{b}-\mathbf{h})|^2. \quad (53)$$

Using the relations $\sum_{\mathbf{h}} |H(\mathbf{b}-\mathbf{h})|^2 = 1$ derived from (*B*3) in Appendix *B*, we have the relation as

$$(1/v)^2 \sum_{\mathbf{h}} |S(\mathbf{b}-\mathbf{h})|^2 = G(\mathbf{b}). \quad (54)$$

By the use of equations (53) and (54), the following results are obtained:

$$I_e(\mathbf{b}) = G(\mathbf{b}) \sum_{\mathbf{h}} |F(\mathbf{h})H(\mathbf{b}-\mathbf{h})|^2 \,[= I_{au}^{HB}(\mathbf{b})], \quad (55)$$

$$I_{eu}(\mathbf{b}) = G(\mathbf{b})|\mathscr{F}_{eu}(\mathbf{b})|^2 = G(\mathbf{b})|\sum_{\mathbf{h}} F(\mathbf{h})H(\mathbf{b}-\mathbf{h})|^2, \quad (56)$$

$$I_{au}(\mathbf{b}) = G(\mathbf{b})|F(\mathbf{b})|^2 \,[= I^{\mathrm{L}}(\mathbf{b})], \quad (57)$$

$$I_a^{IM}(\mathbf{b}) = G(\mathbf{b}) \sum_{\mathbf{h}} |F(\mathbf{b},\mathbf{h})H(\mathbf{b}-\mathbf{h})|^2, \quad (58)$$

$$I_e^J(\mathbf{b}) = G(\mathbf{b})|F(\mathbf{h})H(\mathbf{b}-\mathbf{h})|^2 \quad \text{near point } \mathbf{h}, \quad (59)$$

$$I_{eu}^G(\mathbf{b}) = G(\mathbf{b})|F(\mathbf{h})|^2 \quad \text{near point } \mathbf{h}. \quad (60)$$

Laue function $G(\mathbf{b})$ is a common factor in these formulas; the second terms characterize the feature of each of them.

For a cube-shaped crystal ($N_1 = N_2 = N_3 = 2$) with the cubic structure as treated in § 3, a normalized intensity $J(\xi) = I(\xi 00)/I(000)$ can be expressed, by the use of $f(\xi 00)$ in equation (44), as follows:

$$J(\xi) = \cos^2(\pi\xi).B(\xi), \quad (61)$$

where $B(\xi)$'s are the normalized second terms of equations (55)–(60):

for s.c.

$$B_e(\xi) = \varphi^2(\xi)\{1 + [2\xi/(\pi\alpha^2)]\varphi(\xi)\sin(2\pi\xi) + \sigma(\xi)\sin^2(\pi\xi)\}, \quad (62)$$

$$B_{eu}(\xi) = \varphi^2(\xi)[\cos(\pi\xi) + (\xi/\alpha)\sin(\pi\xi)]^2, \quad (63)$$

$$B_{au}(\xi) = B_a^{IM}(\xi) = B^{\mathrm{L}}(\xi) = \varphi^2(\xi), \quad (64)$$

$$B_e^J(\xi) = \varphi^2(h)\sin^2(\pi\xi)/[\pi^2(\xi-h)^2] \quad \text{near } \xi = h, \quad (65)$$

$$B_{eu}^G(\xi) = \varphi^2(h) \quad \text{near } \xi = h; \quad (66)$$

for b.c.c. and f.c.c.

$$B_e(\xi) = \varphi^2(\xi)\cos^2\left(\frac{\pi\xi}{2}\right)\left[1 + \frac{4\xi}{\pi\alpha^2}\sin(\pi\xi) + 2\sigma(\xi)\sin^2\left(\frac{\pi\xi}{2}\right)\right], \quad (67)$$

$$B_{eu}(\xi) = \varphi^2(\xi)\cos^2\left(\frac{\pi\xi}{2}\right)\left[\cos\left(\frac{\pi\xi}{2}\right) + \frac{\xi}{\alpha}\sin\left(\frac{\pi\xi}{2}\right)\right]^2, \quad (68)$$

$$B_{au}(\xi) = B_a^{IM}(\xi) = B^L(\xi) = \varphi^2(\xi)\cos^2\left(\frac{\pi\xi}{2}\right), \tag{69}$$

$$B_e^J(\xi) = \varphi^2(h)\sin^2(\pi\xi)/[\pi^2(\xi-h)^2] \quad \text{near } \xi = h \text{ even}, \tag{70}$$

$$B_{eu}^G(\xi) = \varphi^2(h) \quad \text{near } \xi = h \text{ even}, \tag{71}$$

in which

$$\sigma(\xi) = \frac{1}{2\pi\alpha}\left[\frac{1}{\varphi(\xi)} + 4 - 8\varphi(\xi)\right], \tag{72}$$

and formulas (*B*1)–(*B*4) in Appendix *B* are used for calculating B_e.

The functions $B(\xi)$ and $J(\xi)$ calculated with $a = 4$ Å, $\gamma = \frac{2}{3}$ Å^2 and $\alpha^2 = 24$ are plotted in Fig. 3. Although all the $B(\xi)$'s have the same value at $\xi = 2$, they have features quite distinct regarding the degree of symmetry with respect to the coordinate $\xi = 2$ and also regarding the sharpness of the curve. B_{eu}^G and B_e^J are symmetric while B_{eu} has a high peak at ξ larger than 2. As expected from the character of each $B(\xi)$, as seen in Fig. 3(*b*) and (*d*), the $J(\xi)$'s show features substantially different from one another with respect to the positions and half-widths of the intensity peaks, though they have all the same values at $\xi = 2$. The difference of $J_{eu}(\xi)$ from $J^L(\xi)$ is the most considerable. The two curves for J_{eu} and J^L are compared for the range $0 \le \xi \le 6{\cdot}5$ in Fig. 4.

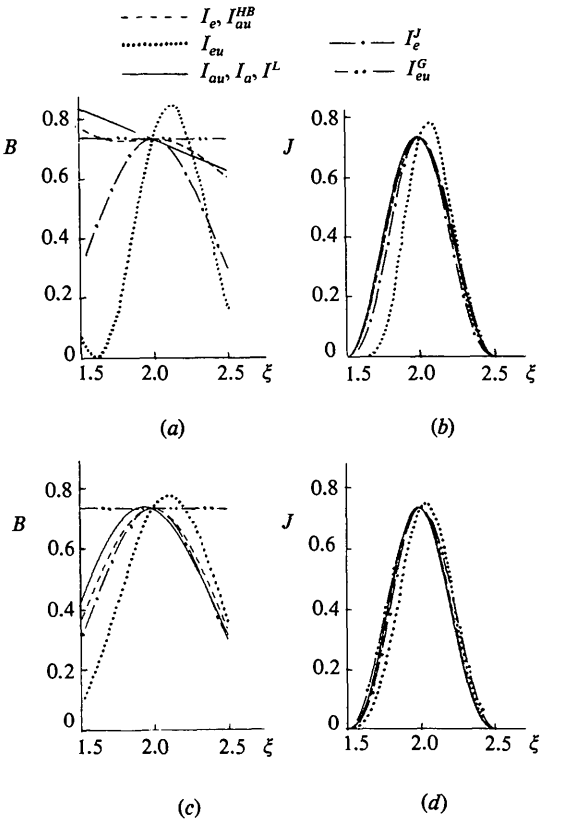

Fig. 3. Comparison of intensity formulas of four types and approximate forms. (*a*) *B* and (*b*) *J* for s.c. and (*c*) *B* and (*d*) *J* for b.c.c. and f.c.c. having cubic shape whose edges are $2a$ (a is the lattice constant).

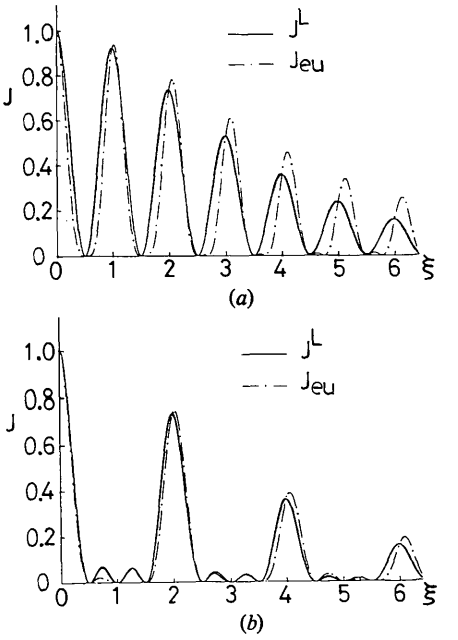

Fig. 4. Comparison of the intensity formulas J^L with J_{eu} (*a*) for a s.c. crystal and (*b*) for b.c.c. and f.c.c. crystals having a cubic shape whose edges are $2a$.

6. Direct-lattice-sum expression

Since the intensity derived in §4 is expressed as a single sum over **h** in the form of $I(\mathbf{b}) = \sum_{\mathbf{h}} \mathscr{I}(\mathbf{b},\mathbf{h})$, it can be rewritten as a single sum over **m** by the use of Poisson's summation formula (Lighthill, 1958) as follows:

$$I(\mathbf{b}) = \sum_{\mathbf{h}} \mathscr{I}(\mathbf{b},\mathbf{h}) = v\sum_{\mathbf{m}} u(\mathbf{b},\mathbf{m}), \tag{73}$$

where

$$u(\mathbf{b},\mathbf{m}) = \int \mathscr{I}(\mathbf{b},\mathbf{b}')\exp(-2\pi i\mathbf{b}'\mathbf{m})\mathrm{d}\mathbf{b}'. \tag{74}$$

Relations necessary for the calculations are

$$\int |S(\mathbf{b})|^2 \exp(-2\pi i\mathbf{b}\mathbf{r})\mathrm{d}\mathbf{b} = \int s(\mathbf{r}')s(\mathbf{r}'+\mathbf{r})\mathrm{d}\mathbf{r}' = \mathscr{V}(\mathbf{r}) = \mathscr{V}(-\mathbf{r}), \tag{75}$$

$$f_\alpha(\mathbf{b})f_\beta^*(\mathbf{b}) = \int [U_\alpha(\mathbf{r}) * U_\beta(-\mathbf{r})]\exp(2\pi i\mathbf{b}\mathbf{r})\mathrm{d}\mathbf{r}, \tag{76}$$

where $\mathscr{V}(\mathbf{r})$ is the volume common to the two boundaries shifted by **r**. By the use of these relations, the

four $I(\mathbf{b})$'s in equations (49)–(52) can be transformed as follows:

$$I_e(\mathbf{b}) = \frac{1}{v}\sum_\alpha\sum_\beta \int [U_\alpha(\mathbf{r}) * U_\beta(-\mathbf{r})] \sum_{\mathbf{m}} \mathscr{V}(\mathbf{r}+\mathbf{m}+\mathbf{r}_\alpha-\mathbf{r}_\beta) \times \exp[2\pi i\mathbf{b}(\mathbf{r}+\mathbf{m}+\mathbf{r}_\alpha-\mathbf{r}_\beta)]d\mathbf{r}, \quad (77)$$

$$I_{eu}(\mathbf{b}) = \frac{1}{v}|\mathscr{F}_{eu}(\mathbf{b})|^2 \sum_{\mathbf{m}} \mathscr{V}(\mathbf{m}) \exp(2\pi i\mathbf{bm}), \quad (78)$$

$$I_{au}(\mathbf{b}) = \frac{1}{v}|F(\mathbf{b})|^2 \sum_{\mathbf{m}} \mathscr{V}(\mathbf{m}) \exp(2\pi i\mathbf{bm}), \quad (79)$$

$$I_a^{IM}(\mathbf{b}) = \frac{1}{v}\sum_\alpha\sum_\beta f_\alpha(\mathbf{b})f_\beta^*(\mathbf{b}) \sum_{\mathbf{m}} \mathscr{V}(\mathbf{m}+\mathbf{r}_\alpha-\mathbf{r}_\beta) \times \exp[2\pi i\mathbf{b}(\mathbf{m}+\mathbf{r}_\alpha-\mathbf{r}_\beta)]. \quad (80)$$

$\mathscr{V}$'s in equations (77)–(80) have the shape effect on the diffraction intensity and restrict the ranges of the summations over $\mathbf{m}$, α and β because $\mathscr{V}(\mathbf{r})$ is zero if $|\mathbf{r}|$ is larger than the crystal size, as seen from equation (75). The smaller the crystal, the less the number of terms to be taken account for the intensity calculation.

The direct-lattice sums in equations (77)–(80) are mathematically identical with the reciprocal-lattice sums in equations (49)–(52), respectively, but the direct-lattice sum is more convenient for smaller crystals.

7. Conclusion

The electron density ρ_a proposed by the present authors is the most adequate and, thus, the intensity expression I_a is the most reliable. The intensity is expressed in alternative ways, one in direct space and the other in reciprocal space; *i.e.*

$$I_a^{IM}(\mathbf{b}) = \left(\frac{1}{v}\right)^2 \sum_{\mathbf{h}} |F(\mathbf{b},\mathbf{h})S(\mathbf{b}-\mathbf{h})|^2 \quad (81)$$

$$= \frac{1}{v}\sum_\alpha\sum_\beta f_\alpha(\mathbf{b})f_\beta^*(\mathbf{b}) \sum_{\mathbf{m}} \mathscr{V}(\mathbf{m}+\mathbf{r}_\alpha-\mathbf{r}_\beta) \times \exp[2\pi i\mathbf{b}(\mathbf{m}+\mathbf{r}_\alpha-\mathbf{r}_\beta)]. \quad (82)$$

The direct-lattice sum is more convenient for a small crystal, while the reciprocal-lattice sum is more advantageous for a large crystal. These forms are successfully applied to the calculation of a number of examples of the intensity profiles for small crystallites. The details are reported in the following paper (Minami & Ino, 1979).

APPENDIX *A*
Random-shift treatment

As a bounded crystal treated in § 2, let us consider the case where the origin O of the lattice does not coincide with the origin O' suitable for describing $s(\mathbf{r})$, and denote $\overrightarrow{O'O} = \mathbf{L}$. In this case, the selection function $z(\mathbf{r})s(\mathbf{r}) = \sum_{\mathbf{m}} s(\mathbf{r})\delta(\mathbf{r}-\mathbf{m})$ used in deriving equations (24)–(27) should be replaced by

$$z(\mathbf{r}-\mathbf{L})s(\mathbf{r}) = \sum_{\mathbf{m}} s(\mathbf{r})\delta(\mathbf{r}-\mathbf{L}-\mathbf{m}). \quad (A1)$$

Thus, the electron density of the shifted crystal can be derived from equations (24)–(27) by replacing $z(\mathbf{r})$ with $z(\mathbf{r}-\mathbf{L})$:

$$\rho_e(\mathbf{r},\mathbf{L}) = \sum_\alpha [U_\alpha(\mathbf{r}) * z(\mathbf{r}-\mathbf{L}-\mathbf{r}_\alpha)]s(\mathbf{r}), \quad (A2)$$

$$\rho_{eu}(\mathbf{r},\mathbf{L}) = \rho_e^{\text{cell}}(\mathbf{r}) * [z(\mathbf{r}-\mathbf{L})s(\mathbf{r})], \quad (A3)$$

$$\rho_{au}(\mathbf{r},\mathbf{L}) = \rho_e^{\text{cell}}(\mathbf{r}) * [z(\mathbf{r}-\mathbf{L})s(\mathbf{r})], \quad (A4)$$

$$\rho_a(\mathbf{r},\mathbf{L}) = \sum_\alpha U_\alpha(\mathbf{r}) * [z(\mathbf{r}-\mathbf{L}-\mathbf{r}_\alpha)s(\mathbf{r})]. \quad (A5)$$

By the use of equation (36) and $\Phi(\mathbf{b},\mathbf{h})$ in equation (38), the amplitude derived from $\rho(\mathbf{r},\mathbf{L})$ is found to be:

$$A(\mathbf{b},\mathbf{L}) = \sum_{\mathbf{h}} \Phi(\mathbf{b},\mathbf{h}) \exp(2\pi i\mathbf{hL}), \quad (A6)$$

from which the corresponding intensity is:

$$I(\mathbf{b},\mathbf{L}) = A(\mathbf{b},\mathbf{L})A^*(\mathbf{b},\mathbf{L}) = \sum_{\mathbf{h}} |\Phi(\mathbf{b},\mathbf{h})|^2 + \sum_{\mathbf{h}\neq\mathbf{h}'}\sum \Phi(\mathbf{b},\mathbf{h})\Phi^*(\mathbf{b},\mathbf{h}') \exp[2\pi i(\mathbf{h}-\mathbf{h}')\mathbf{L}]. \quad (A7)$$

In this expression, it is found that $I(\mathbf{b},\mathbf{L})$ shows the same periodicity as that of the lattice with respect to $\mathbf{L}$.

A set of lattice points in an unshifted crystal, another set of those in the crystal shifted by $\mathbf{L}$ and their superposition are shown in Figs. 5(*a*), (*b*) and (*c*) respectively. Even for the crystal specified by a given shape function, as seen from the figures, the number and arrangement of lattice points in the crystal generally vary with the value of $\mathbf{L}$, retaining the lattice periodicity. The variation of the point set takes place relating to points near the boundary; the lattice points in the vicinity of the center O make a common set to all crystals independently of the vector $\mathbf{L}$.

For the actual crystalline sample composed of small crystals with a definite shape, $\mathbf{L}$ may be considered to vary from crystal to crystal with some probability, so

that the intensity from the sample should be statistically averaged. Although this probability is difficult to estimate in general, it may be practical to assume simply that the probability is uniform, *i.e.* **L** occurs randomly. In this case the intensity may be averaged with respect to the 'random shift' of **L** over one period of the lattice. By this treatment, the last term in $I(\mathbf{b},\mathbf{L})$ in equation (*A*7) is found to vanish and we have

$$I(\mathbf{b}) = (1/v)\int_{[v]} I(\mathbf{b},\mathbf{L})\mathrm{d}\mathbf{L} = \sum_{\mathbf{h}} |\Phi(\mathbf{b},\mathbf{h})|^2, \qquad (A8)$$

which is the same as the first term in equation (48). Thus, the intensity expressed by the double sum over **h** and **h**′ is reduced to that of a single sum over **h** by this 'random-shift treatment'.

For a large crystal, since the number of atoms near the surface is small compared with that in the common set of atoms near the center, the change in **L** has only a negligible effect on the intensity. On the other hand, for an extremely small crystal the effect of **L** becomes appreciable. When 'the random-shift treatment' mentioned above is applied, the same intensity form given in equation (*A*8) is obtained for small as well as large crystals.

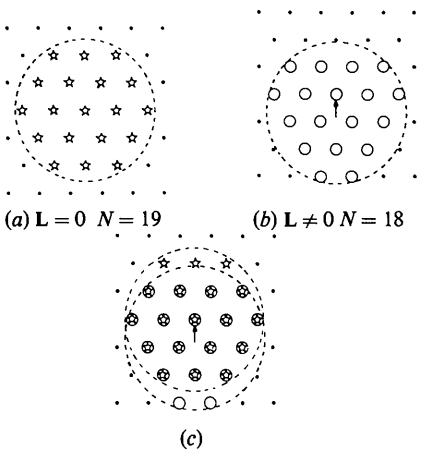

Fig. 5. Sets of lattice points specified by (*a*) **L** = 0 and (*b*) **L** ≠ 0 for a disk-shaped crystal. *N* is the number of lattice points inside the boundary specified by $s(\mathbf{r})$. (*c*) The superposition of the above two sets. Asterisks and open circles show the lattice points inside the circular boundary for **L** = 0 and **L** ≠ 0 respectively. Small points show lattice points outside the boundary. Broken lines show the circular boundaries.

APPENDIX *B*
Mathematical formulas

$$\sum_{h=-\infty}^{\infty} \frac{1}{\alpha - h} = \pi\cot(\pi\alpha), \qquad (B1)$$

$$\sum_{h=-\infty}^{\infty} \frac{1}{\alpha^2 + h^2} = \left(\frac{\pi}{\alpha}\right)\coth(\pi\alpha) \simeq \frac{\pi}{\alpha} \text{ for } \alpha > 2, \qquad (B2)$$

$$\sum_{h=-\infty}^{\infty} \frac{1}{(\alpha - h)^2} = \frac{\pi^2}{\sin^2(\pi\alpha)}, \qquad (B3)$$

$$\sum_{h=-\infty}^{\infty} \frac{1}{(\alpha^2 + h^2)^2} = \frac{\pi}{2\alpha^3}\left[\coth(\pi\alpha) + \frac{\pi\alpha}{\sinh^2(\pi\alpha)}\right] \simeq \frac{\pi}{2\alpha^3} \quad \text{for } \alpha > 2. \qquad (B4)$$

References

EWALD, P. P. (1940). *Proc. Phys. Soc. London*, **52**, 167–174.

GUINIER, A. (1963). *X-ray Diffraction*, pp. 90–93. San Francisco: Freeman.

HOSEMANN, R. & BAGCHI, S. N. (1962). *Direct Analysis of Diffraction by Matter*, pp. 260–264. Amsterdam: North-Holland.

JAMES, R. W. (1954). *The Optical Principles of the Diffraction of X-rays. The Crystalline State.* II, pp. 548–550. London: Bell.

LAUE, M. VON (1936). *Ann. Phys. (Paris)*, **26**, 55–68.

LIGHTHILL, M. J. (1958). *An Introduction to Fourier Analysis and Generalized Function*, pp. 67–71. Cambridge Univ. Press.

MINAMI, N. & INO, T. (1979). *Acta Cryst.* A**35**, 171–176.

PATTERSON, A. L. (1939). *Phys. Rev.* **56**, 972–977.